J|A|C|S
ARTICLES
Published on Web 06/06/2006

Toward Exceeding the Shockley−Queisser Limit: Photoinduced Interfacial Charge Transfer Processes that Store Energy in Excess of the Equilibrated Excited State

Paul G. Hoertz,[†] Aaron Staniszewski,[†] Andras Marton,[†] Gerard T. Higgins,[†] Christopher D. Incarvito,[‡] Arnold L. Rheingold,[‡] and Gerald J. Meyer*,[†]

Contribution from the Departments of Chemistry and Materials Science and Engineering, Johns Hopkins University, 3400 North Charles Street, Baltimore, Maryland 21218, and Department of Chemistry and Biochemistry, University of California, San Diego, 9500 Gilman Drive, La Jolla, California 92093-0358

Received January 31, 2006; E-mail: meyer@jhu.edu

Abstract: Nanocrystalline (anatase), mesoporous TiO_2 thin films were functionalized with $[Ru(bpy)_2(deebq)](PF_6)_2$, $[Ru(bq)_2(deeb)](PF_6)_2$, $[Ru(deebq)_2(bpy)](PF_6)_2$, $[Ru(bpy)(deebq)(NCS)_2]$, or $[Os(bpy)_2(deebq)](PF_6)_2$, where bpy is 2,2′-bipyridine, bq is 2,2′-biquinoline, and deeb and deebq are 4,4′-diethylester derivatives. These compounds bind to the nanocrystalline TiO_2 films in their carboxylate forms with limiting surface coverages of $8 (\pm 2) \times 10^{-8}$ mol/cm^2. Electrochemical measurements show that the first reduction of these compounds (−0.70 V vs SCE) occurs prior to TiO_2 reduction. Steady state illumination in the presence of the sacrificial electron donor triethylamine leads to the appearance of the reduced sensitizer. The thermally equilibrated metal-to-ligand charge-transfer excited state and the reduced form of these compounds do not inject electrons into TiO_2. Nanosecond transient absorption measurements demonstrate the formation of an extremely long-lived charge separated state based on equal concentrations of the reduced and oxidized compounds. The results are consistent with a mechanism of ultrafast excited-state injection into TiO_2 followed by interfacial electron transfer to a ground-state compound. The quantum yield for this process was found to increase with excitation energy, a behavior attributed to stronger overlap between the excited sensitizer and the semiconductor acceptor states. For example, the quantum yields for $[Os(bpy)_2(dcbq)]/TiO_2$ were $\phi(417\text{ nm}) = 0.18 \pm 0.02$, $\phi(532.5\text{ nm}) = 0.08 \pm 0.02$, and $\phi(683\text{ nm}) = 0.05 \pm 0.01$. Electron transfer to yield ground-state products occurs by lateral intermolecular charge transfer. The driving force for charge recombination was in excess of that stored in the photoluminescent excited state. Chronoabsorption measurements indicate that ligand-based intermolecular electron transfer was an order of magnitude faster than metal-centered intermolecular hole transfer. Charge recombination was quantified with the Kohlrausch−Williams−Watts model.

Introduction

The maximum solar-to-electrical energy conversion efficiency from a single junction photovoltaic cell is about 31% (1 sun, air mass 1.5 spectral distribution).[1] This celebrated limit was first calculated by Shockley and Queisser under the assumption that solar photons with energy larger than the semiconductor band gap, E_g, lose all energy in excess of E_g.[1] The theoretical efficiency exceeds 60% when electron−hole pairs are converted to electrical power prior to band edge thermalization.[2] Attempts to fabricate such "hot carrier" solar cells have thus far been unsuccessful, but may be enabled by recent demonstrations that a single photon can create multiple electron hole pairs in semiconductor nanoparticles.[3−5] However, the recent demonstration that multiple electron-hole pairs can be generated in a semiconductor nanoparticle after absorption of a single photon represents a significant advance.[3−5]

The Shockley−Queisser limit also applies to molecular solar cells. Here too the realization of >31% efficiencies requires that energy stored in molecular excited states be collected prior to vibrational relaxation to the lowest electronic state. Relatively few strategies for accomplishing this exist.[6,7] Vibrational relaxation in inorganic and organic excited states is known to occur on ultrafast time scales. Therefore, any successful strategy would require subpicosecond charge-transfer processes.

The recent demonstrations of ultrafast interfacial electron transfer and rapid charge trapping at dye-sensitized TiO_2 interfaces may provide unanticipated opportunities for exceeding the Shockley−Queisser limit.[8−16] Indeed, there is experimental

[†] Johns Hopkins University.
[‡] University of California, San Diego.

(1) Shockley, W.; Queisser, H. J. *J. Appl. Phys.* **1961**, *32*, 510.
(2) Ross, R. T.; Nozik, A. J. *J. Appl. Phys.* **1982**, *53*, 3813.
(3) Schaller, R.; Klimov, V. *Phys. Rev. Lett.* **2004**, *92*, 186601.
(4) Ellingson, R. J.; Beard, M. C.; Johnson, J. C.; Yu, P.; Micic, O. I.; Nozik, A. J.; Shabaev, A.; Efros, A. L. *Nanolett.* **2005**, 5, 865.
(5) Nozik, A. J. *Inorg. Chem.* **2005**, *44*, 6893.
(6) (a) Becker, R. S.; Donlan, E.; Balke, D. E. *J. Chem. Phys.* **1969**, *50*, 239. (b) Becker, R. S.; Pellicciolo, A. P.; Romani, A.; Favaro, G. *J. Am. Chem. Soc.* **1999**, *121*, 2104.
(7) (a) Koval, C. A.; Segar, P. R. *J. Am. Chem. Soc.* **1989**, *111*, 2001. (b) Koval, C. A.; Segar, P. R. *J. Phys. Chem.* **1990**, *94*, 203.

10.1021/ja060470e CCC: $33.50

Scheme 1

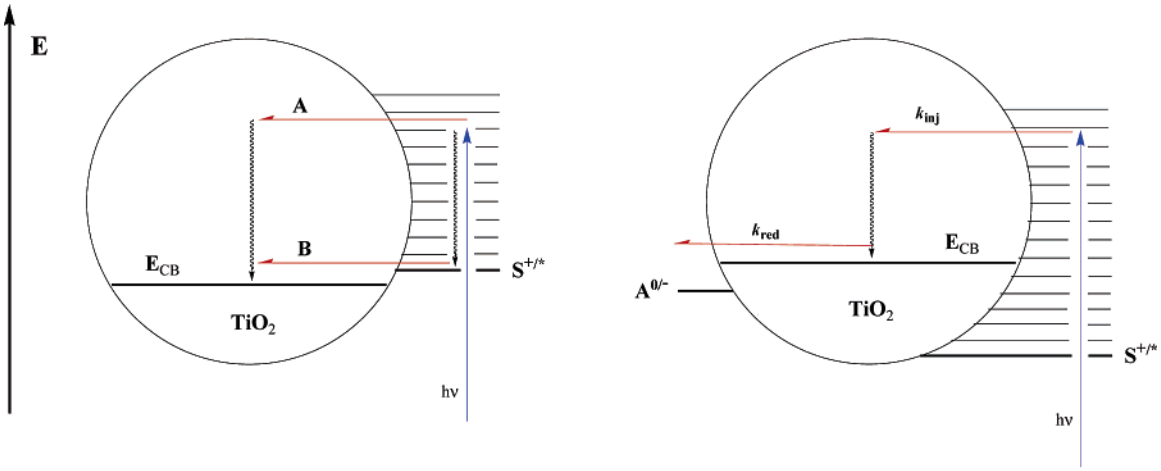

evidence for excited state electron injection from the initially formed Franck−Condon state, i.e., interfacial electron transfer without vibrational energy loss in the photoexcited dye.[9] However, whether such ultrafast electron injection is beneficial, or even necessary, for efficient energy conversion in regenerative dye-sensitized solar cells remains unknown.[17] Quantitative injection would be expected from the long-lived metal-to-ligand charge transfer (MLCT) excited states of the commonly utilized Ru(II) polypyridyl sensitizers even if the rate constant was slowed by ∼3 orders of magnitude.[18]

Complete excited state quenching, electron transfer rate constants, and interfacial energetics reported in the literature strongly suggest that the conduction band edge, E_{cb}, lies below the reduction potential of the thermally equilibrated excited (thexi) state, $S^{+/*}$, in regenerative dye-sensitized solar cells, Scheme 1, left hand side.[18] Therefore, it matters little whether the Franck−Condon state (path A) or the thermally equilibrated excited state (path B) injects the electron. Loss of the excess energy occurs on one side of the interface or the other: phonon release in the solid or nonradiative decay of the excited state. Both pathways ultimately yield the same thermalized products, a conduction band electron and an oxidized dye.

Herein we describe novel molecular charge separation processes that ultimately store more free energy than the thexi state. Our approach exploits ultrafast dye-sensitized electron injection into TiO_2 nanocrystallites followed by electron transfer to a molecular acceptor that would not be reduced by the thermally equilibrated excited state. The interfacial energetics shown on the right-hand side of Scheme 1, coupled with the well-known ultrafast injection,[8−16] are indeed expected to give rise to such a semiconductor-mediated charge transfer pathway. Since the acceptors are reduced only when electrons are injected from upper vibrational excited states, their reduction serves as a direct probe of "hot electron" involvement in interfacial phenomena.[19,20] The studies reported here represent proof-of-principle examples of this behavior.

Experimental Section

Materials. Tetrabutylammonium perchlorate (Fluka), acetonitrile (Burdick and Jackson), ethanol (Pharmco), $RuCl_3 \cdot xH_2O$ (Alfa Aesar), $OsCl_3 \cdot xH_2O$ (Alfa Aesar), lithium iodide (Alfa Aesar), and 4,4′-dicarboxylic acid-2,2′-biquinoline ($dcbqH_2$, Fluka) were used as received. Acetone, sulfuric acid, nitric acid, potassium dichromate, 2,2′-biquinoline (bq), 2,2′-bipyridine (bpy), LiCl, trifluoromethanesulfonic acid, dichlorobenzene, dimethyl formamide, methylene chloride, chloroform, tetrabutylammonium thiocyanate, tetrabutylammonium iodide, ammonium hexafluorophosphate, and $[Ru(bpy)_3](Cl)_2$ were purchased from Aldrich and were reagent grade or better.

Synthesis. 4,4′-Dicarboxylic acid-2,2′-bipyridine ($dcbH_2$). 4,4′-Dimethyl-2,2′-bipyridine (5.0 g) in heated H_2SO_4 (125 mL, 70−80 °C) was oxidized by adding solid potassium dichromate (24 g) slowly. The temperature was held consistently between 70 and 80 °C during the transfer. The deep green mixture was then poured over 800 mL of ice/H_2O, affording a light yellow precipitate that was isolated by vacuum filtration and was washed with H_2O. The solid was then refluxed in 50% HNO_3 (150 mL) for 4 h. The cooled solution was then poured over ice and diluted with 800 mL of H_2O. A white powder was isolated by vacuum filtration and washed with H_2O (5.99 g, 90%).[21]

4,4′-Diethylester-2,2′-bipyridine (deeb). This ligand was synthesized from $dcbH_2$ by a literature preparation.[22] ^{1}H NMR δ (CD_2Cl_2): 8.93 (2H, dd), 8.85 (2H, dd), 7.89 (2H, dd), 4.44 (4H, q, CH_2), 1.44 (6H, t, CH_3).

(8) Tachibana, Y.; Moser, J. E.; Grätzel, M.; Klug, D. R.; Durrant, J. *J. Phys. Chem. B* **1996**, *100*, 20056.
(9) Hannappel, T.; Burfeindt, B.; Storck, W.; Willig, F. *J. Phys. Chem. B* **1997**, *101*, 6799.
(10) (a) Heimer, T. A.; Heilweil, E. J. *J. Phys. Chem. B* **1997**, *101*, 10990. (b) Heimer, T. A.; Heilweil, E. J.; Bignozzi, C. A.; Meyer, G. J. *J. Phys. Chem. A* **2000**, *104*, 4256.
(11) Ellingson, R. J.; Asbury, J. B.; Ferrere, S.; Ghosh, H. N.; Sprague, J. R.; Lian, T.; Nozik, *J. Phys. Chem. B* **1997**, *101*, 6455.
(12) Piotrowiak, P.; Galoppini, E.; Wei, Q.; Meyer, G. J.; Wiewior, P. *J. Am. Chem. Soc.* **2003**, *125*, 5278.
(13) (a) Benko, G.; Kallioinen, J.; Korppi-Tommola, J. E. I.; Yartsev, A. P.; Sundstrom, V. *J. Am. Chem. Soc.* **2002**, *124*, 489. (b) Benko, G.; Myllyperkio, P.; Pan, J.; Yartsev, A. P.; Sundstrom, V. *J. Am. Chem. Soc.* **2003**, *125*, 1118. (c) Kallioinen, J.; Benko, G.; Sundstrom, V.; Korppi-Tommola, J. E. I.; Yartsev, A. P. *J. Phys. Chem. B* **2002**, *106*, 4396.
(14) Kuciauskas, D.; Monat, J. E.; Villahermosa, R.; Gray, H. B.; Lewis, N. S.; McCusker, J. K. *J. Phys. Chem. B* **2002**, *106*, 9347.
(15) (a) Asbury, J. B.; Hao, E.; Wang, Y.; Lian, T. *J. Phys. Chem. B* **2000**, *104*, 11957. (b) Asbury, J. B.; Hao, E.; Wang, Y. Q.; Ghosh, H. N.; Lian, T. Q. *J. Phys. Chem. B* **2001**, *105*, 4545.
(16) Hoertz, P. G.; Thompson, D. W.; Friedman, L. A.; Meyer, G. J. *J. Am. Chem. Soc.* **2002**, *124*, 9690.
(17) Haque, S. A.; Palomeras, E.; Cho, B. M.; Green, A. N. M.; Hirata, N.; Klug, D. R.; Durrant, J. R. *J. Am. Chem. Soc.* **2005**, *127*, 3456.
(18) (a) Grätzel, M. *Nature* **2001**, *414*, 338. (b) Watson, D. F.; Meyer, G. J. *Annu. Rev. Phys. Chem.* **2005**, *56*, 119.
(19) (a) Ferrere, S.; Gregg, B. A. *J. Am. Chem. Soc.* **1998**, *120*, 843. (b) Islam, A.; Hara, K.; Singh, L. P.; Katoh, R.; Yanagida, M.; Murata, S.; Takahashi, Y.; Sugihara, H.; Arakawa, H. *Chem. Lett.* **2000**, 490. (c) Moser, J. E.; Grätzel, M. *Chimia* **1998**, *52*, 160.
(20) Huber, R.; Sporlein, S.; Moser, J. E.; Grätzel, M.; Wachtveitl, J. *J. Phys. Chem. B* **2000**, *104*, 8995.
(21) Oki, A. R.; Morgen, R. J. *Synth. Commun.* **1995**, *25*, 4093.
(22) Maerker, G.; Case, F. H. *J. Am. Chem. Soc.* **1958**, *80*, 2747.

4,4′-Dicarboxylato-2,2′-bipyridine Disodium Salt (dcb(Na)$_2$). A solid sample of dcbH$_2$ (1.04 g) was added to 20 mL of deionized H$_2$O and treated with NaOH (aq) (25% w/v) until the solid was completely dissolved. During this process, the pH increased from 3 to 9. Acetone (700 mL) was then added to precipitate out dcb(Na)$_2$ (1.21 g, 99%).

4,4′-Diethylester-2,2′-biquinoline (deebq). A 10 g sample of dcbqH$_2$ was added to 360 mL of stirred EtOH and was then chilled in an ice/H$_2$O bath. Sulfuric acid (92 mL) was slowly added. The suspension was refluxed for 27 h; 1 h into the reflux, the ligand completely dissolved. Neutralization with NaOH (aq, 25% w/v) led to precipitation of a yellow solid, which was filtered and dried in an oven. The solid was dissolved in methylene chloride, filtered, and placed on a rotoevaporator to remove the methylene chloride (9.7 g, 84%). ^{1}H NMR δ ($CDCl_3$): 9.35 (2H, s), 8.80 (2H, d), 8.35 (2H, d), 7.85 (2H, td), 7.70 (2H, td), 4.60 (4H, q, CH_2), 1.55 (6H, t, CH_3).

4,4′-Dicarboxylato-2,2′-biquinoline Disodium Salt (dcbq(Na)$_2$). About 5 g of dcbqH$_2$ was added to 50 mL of deionized H$_2$O and treated with NaOH (aq) (25% w/v) until the solid was completely dissolved. During this process, the pH increased from 5 to 8. Acetone (750 mL) was then added to precipitate dcbq(Na)$_2$ (95%).

[Ru(bpy)$_2$(deebq)](PF$_6$)$_2$. (a) Ru(bpy)$_2$Cl$_2$ was synthesized according to a literature preparation.[23] UV−vis (CH_2Cl_2), nm: 380, 557. (b) Ru(bpy)$_2$(OTf)$_2$ (where OTf is trifluoromethanesulfonate) was prepared by adding Ru(bpy)$_2$Cl$_2$ (1.67 g) to 150 mL of argon-purged *o*-dichlorobenzene. Trifluoromethanesulfonic acid (HOTf, 1 mL) was added to the suspension, and the reaction mixture immediately turned from purple to red. After 1 h of gentle stirring, the solution was filtered and a brick-red precipitate was washed with copious amounts of ether to isolate Ru(bpy)$_2$(OTf)$_2$, in 97% yield (2.28 g).[24] ^{1}H NMR δ (CH_3CN): 9.33 (2H, dd), 8.51 (2H, d), 8.39 (2H, d), 8.25 (2H, td), 7.94 (2H, td), 7.87 (2H, m), 7.60 (2H, d), 7.30 (2H, m). (c) Ru(bpy)$_2$(OTf)$_2$ (0.5 g, 0.7 mmol) was dissolved in dry acetone (150 mL) with deebq (360 mg, 0.9 mmol) and was refluxed under argon for 1 day. The acetone was removed by rotoevaporation. The red solid was treated with deionized H$_2$O (80 mL), and the solution was filtered. The filtrate was treated with 2 M NH_4PF_6 (aq, 5 mL) to afford a red precipitate, which was washed with H$_2$O followed by ether. After drying in an oven at 75 °C, the solid was dissolved in 10 mL of acetone and placed in an ether chamber for slow vapor diffusion recrystallization. This afforded good crystals (50 mg, 14%). ^{1}H NMR δ (CD_3CN): 8.97 (2H, s), 8.69 (2H, dd), 8.42 (4H, dd), 8.06 (4H, m), 7.77 (4H, m), 7.69 (2H, m), 7.36 (6H, m), 7.2 (2H, d), 4.59 (4 H, q, CH_2), 1.51 (6H, t, CH_3). Elem. Anal. Calcd: C, 46.71; H 3.40; N, 7.43. Found: C, 48.44; H, 3.43; N, 7.74. FAB-MS: Calcd for (M − PF_6) 958.8, found 958.8; Calcd for (M − 2PF_6) 813.8, found 814.0.

[Os(bpy)$_2$(deebq)](PF$_6$)$_2$. (a) Os(bpy)$_2$Cl$_2$ was prepared according to a modified literature preparation.[25] LiCl (0.95 g) and bpy (0.48 g) were added to argon-purged DMF (25 mL) followed by $OsCl_3 \cdot xH_2O$ (0.52 g). The solution was refluxed under argon for 2.5 h and then allowed to cool to room temperature. The reaction solution was refluxed for an additional hour under argon in the presence of 1 mL of triethylamine, cooled to room temperature, poured over 100 mL of dry acetone, and cooled to −5 °C overnight. Filtration yielded a purple-brown solid (450 mg, 52%). ^{1}H NMR δ (d_6-DMSO): 9.67 (2H, d), 8.59 (2H, dd), 8.38 (2H, dd), 7.59 (4H, m), 7.30 (4H, t), 7.56 (2H, td). (b) Os(bpy)$_2$(OTf)$_2$ was prepared by addition of Os(bpy)$_2$Cl$_2$ (440 mg) to 125 mL of argon-purged *o*-dichlorobenzene. Trifluoromethanesulfonic acid (HOTf, 0.75 mL) was added to the suspension, and the reaction mixture immediately turned from purple to red. After stirring for 1 h, the reaction solution was filtered to isolate a dark green precipitate that was washed with copious amounts of ether (320 mg, 52%).[24] ^{1}H NMR δ (CH_3CN): 9.26 (2H, d), 8.51 (2H, d), 8.37 (2H, d), 7.95 (2H, td), 7.88 (4H, m), 7.56 (2H, d), 7.18 (2H, m). (c) [Os(bpy)$_2$(OTf)$_2$] (250 mg, 0.31 mmol) and deebq (1.15 g, 2.87 mmol) were dissolved in dry acetone (10 mL) and refluxed for 2 days under argon. Upon cooling to room temperature, the acetone was removed by rotoevaporation. The solid was added to 50 mL of methylene chloride and filtered, and the methylene chloride was removed under a vacuum. The resultant solid was dissolved in acetone (50 mL) and filtered. The slow addition of diethyl ether (200 mL) resulted in precipitation of the desired product. Recrystallization from acetone was repeated 4 times with 10 mL of acetone and 40 mL of ether. The filtrate in each case was brown-green in color; after the last recrystallization, the filtrate was dark green with no hints of brown. The black solid was dissolved in 15 mL of acetone. After the solution was filtered, the filtrate was treated with 15 mL of deionized H$_2$O. Dropwise addition of 2 M NH_4PF_6 (aq, 5 mL) led to precipitation of a black solid. After adding 20 mL of deionized H$_2$O, the solid was isolated via filtration and washed with H$_2$O followed by ether. After drying in an oven at 75 °C, the solid was dissolved in 10 mL of acetone and placed in an ether chamber for slow vapor diffusion recrystallization. This afforded good crystals (50 mg, 14%). ^{1}H NMR δ (CD_3CN): 8.90 (2H, s), 8.69 (2H, dd), 8.42 (4H, dd), 7.90 (4H, m), 7.63 (4H, m), 7.49 (2H, d), 7.40 (2H, td), 7.23 (4H, m), 6.87 (2H, d), 4.44 (4 H, q, CH_2), 1.51 (6H, t, CH_3). Elem. Anal. Calcd: C, 44.30; H 3.04; N, 7.05. Found: C, 45.22; H 3.32; N, 6.90. MALDI-MS: Calcd for (MH^+), 904; found, 904.

[Ru(bq)$_2$(deeb)](PF$_6$)$_2$. (a) Ru(bq)$_2$Cl$_2$ was synthesized using the literature procedure for Ru(bpy)$_2$Cl$_2$ (67%).[23] UV−vis ($CHCl_3$), nm: 431, 650 (sh), 737. (b) Ru(bq)$_2$Cl$_2$ (0.5 g, 0.7 mmol) and deeb (0.32 g, 1.1 mmol) were added to 4:1 EtOH/H$_2$O (10 mL) and refluxed under argon for 24 h protected from room light using aluminum foil. After cooling to room temperature, the reaction solution was treated with 20 mL of deionized H$_2$O and then filtered to remove any excess free ligand. The reaction solution was treated with 2 M NH_4PF_6 (aq, 5 mL) giving a precipitate that was filtered and washed with H$_2$O followed by ether. The solid was dissolved in a minimal amount of dry acetone and recrystallized by slow ether addition with stirring. This recrystallization was performed repetitively until the acetone/ether filtrates were clear, approx 3−4 times (70 mg, 9%). ^{1}H NMR δ (CD_3CN): 9.00 (4H, q), 8.82 (2H, d), 8.49 (2H, d), 8.13 (6H, m), 7.85 (4H, m), 7.52 (2H, m), 7.37 (4H, m), 7.06 (4H, m), 6.94 (2H, m), 4.32 (4 H, q, CH_2), 1.31 (6H, t, CH_3). Elem. Anal. Calcd: C, 51.88; H, 3.35; N, 6.95. Found: C, 50.94; H, 4.27; N, 6.85. FAB-MS: Calcd for (M − 2PF_6) 914.0, found 914.4; Calcd for (M − 2PF_6 − bq) 657.7, found 658.1.

[Ru(bpy)(deebq)$_2$](PF$_6$)$_2$. (a) Ru(deebq)$_2$Cl$_2$ was synthesized using the following procedure. $RuCl_3 \cdot xH_2O$ (0.2 g), deebq (0.7 g, 1.8 mmol), and LiCl (0.42 g, 9.9 mmol) were added to argon-purged 1:1 EtOH/$CHCl_3$ (20 mL) and refluxed under argon for 16 h. After cooling to room temperature, ascorbic acid (0.22 g, 1.2 mmol) was added, and the brown reaction solution was refluxed again under argon for 3 h, during which time the reaction solution turned dark green. Upon cooling to room temperature, the reaction solution was rotoevaporated to remove most of the $CHCl_3$. The solution was transferred to a filter using deionized H$_2$O, and the resulting black solid was washed with copious amounts of H$_2$O followed by ether (0.65 g, 80%). UV−vis (CH_2Cl_2), nm: 464, 676, 750 (sh). (b) [Ru(bpy)(deebq)$_2$](PF$_6$)$_2$ was prepared using the following procedure. Ru(deebq)$_2$Cl$_2$ (1.6 g, 1.7 mmol) was added to argon purged EtOH (100 mL). Silver(I) hexafluorophosphate (1.25 g, 5 mmol) dissolved in 5 mL of argon purged EtOH was then added, producing a deep blue reaction solution. The reaction solution was refluxed under argon for 1 h and cooled to room temperature. After 100 mL of argon purged deionized H$_2$O and bpy (2.57 g, 16.5 mmol) were added, the reaction solution was refluxed for 24 h under argon and protected from room light using aluminum foil. Upon cooling to room temperature, the purple reaction solution was filtered; the filtrate was treated with 2 M NH_4PF_6 (aq, 10 mL), giving a precipitate that was filtered and washed with H$_2$O until the washings were clear. The purple solid was then dissolved in acetonitrile and was filtered. After rotoevaporation of the acetonitrile, the purple solid was dissolved in

(23) Sullivan, B. P.; Salmon, D. J.; Meyer, T. J. *Inorg. Chem.* **1978**, *17*, 3334.
(24) Lay, P. A.; Sargerson, A. M.; Taube, H. *Inorg. Synth.* **1986**, *24*, 291.
(25) Geno, M. J. K.; Dawson, J. H. *Inorg. Chim. Acta* **1985**, *97*, 241.

dry acetone, the solution was filtered, and the purple solution was placed in an ether chamber for slow recrystallization (0.46 g, 21%). ^{1}H NMR δ (CD_3CN): 9.38 (2H, s), 9.22 (2H, s), 8.74 (2H, d), 8.51 (2H, d), 7.85 (2H, d), 7.75 (2H, t), 7.60 (4H, m), 7.45 (4H, m), 7.30 (2H, d), 7.15 (4H, m), 7.00 (2H, m), 4.70 (4 H, q, CH_2), 4.60 (4 H, q, CH_2), 1.60 (6H, t, CH_3), 1.50 (6H, t, CH_3). Elem. Anal. Calcd: C, 51.68; H, 3.59; N, 6.23. Found: C, 50.47; H, 3.66; N, 6.07.

[Ru(bpy)(deebq)(NCS)$_2$]. (a) $[Ru(bpy)(deebq)_2](PF_6)_2$ (0.17 g, 0.13 mmol) was dissolved in 80 mL of acetonitrile and irradiated (1000 W Xe lamp, $\lambda > 570$ nm) in a 100 mL borosilicate round-bottomed flask under argon for 4 days.[26] Complete conversion to $[Ru(bpy)(deebq)(CH_3CN)_2](PF_6)_2$ was apparent from UV−vis spectra. The acetonitrile was removed, and the resultant red solid was dissolved in 15 mL of dry acetone that was treated with 15 mL of H_2O. The deebq ligand was removed by filtration. The filtrate was then treated with 2 M NH_4PF_6 (aq, 5 mL), giving a red precipitate, which was filtered and washed with H_2O followed by ether (0.11 g, 80%). ^{1}H NMR δ (CD_3CN): 9.75 (1H, dd), 9.05 (3H, m), 8.80 (1H, s), 8.70 (1H, d), 8.20 (2H, m), 8.00 (4H, m), 7.85 (1H, m), 7.77 (1H, d), 7.70 (1H, m), 7.50 (1H, m), 7.25 (1H, m), 7.00 (1H, d), 4.75 (4H, q, CH_2), 4.55 (4H, q, CH_2), 2.60 (3H, s, CH_3CN−Ru), 2.40 (3H, s, CH_3CN−Ru), 1.60 (6H, t, CH_3), 1.50 (6H, t, CH_3). UV−vis (CH_3CN), nm: 490 (sh), 525. (b) $[Ru(bpy)(deebq)(CH_3CN)_2](PF_6)_2$ (40 mg) was dissolved in argon purged EtOH (5 mL) containing tetrabutylammonium thiocyanate (25 mg) and refluxed for 4 h, during which time, a blue-green precipitate formed. The solid was isolated by filtration and rinsed with EtOH and ether (13 mg, 43%). ^{1}H NMR δ (CD_3CN): 9.49 (1H, d), 9.33 (1H, d), 8.98 (1H, dd), 8.89 (1H, s), 8.74 (1H, d), 8.72 (1H, s), 8.14 (1H, d), 8.00 (3H, m), 7.90 (1H, m), 7.75 (1H, m), 7.66 (1H, td), 7.55 (1H, m), 7.36 (1H, d), 7.25 (2H, m), 7.00 (1H, m), 4.66 (2H, q, CH_2), 4.54 (2H, q, CH_2), 1.59 (3H, t, CH_3), 1.50 (3H, t, CH_3). ATR−IR: 2095 cm^{-1} and 2071 cm^{-1} (N═C═S).

[Ru(bpy)$_2$(dcbq)]. $Ru(bpy)_2Cl_2\cdot 2H_2O$ (54 mg, 0.10 mmol) and $dcbq(Na)_2$ (70 mg, 0.18 mmol) were added to N_2-saturated deionized H_2O (5 mL). Refluxing under N_2 for 8 h resulted in the formation of a brick-red precipitate that was filtered and washed with deionized H_2O followed by acetone (69 mg, 88%). ^{1}H NMR δ (d_6-DMSO): 8.16 (6H, m), 8.03 (2H, s), 7.54 (4H, t), 7.32 (4H, t), 6.92 (6H, m), 6.53 (2H, td), 6.41 (2H, d).

[Os(bpy)$_2$(dcbq)]. $Os(bpy)_2Cl_2\cdot 2H_2O$ (33 mg, 0.052 mmol) and $dcbq(Na)_2$ (70 mg, 0.20 mmol) were added to N_2-saturated deionized H_2O (5 mL). After refluxing under N_2 for 8 h, the reaction solution was filtered (removing a black solid), and acetone (250 mL) was added to the filtrate. The solution was cooled in a freezer for 4 days, over which time the desired product precipitates out as a black solid. The product was isolated by vacuum filtration and washed with deionized H_2O and acetone (10 mg, 20%). ^{1}H NMR δ (d_6-DMSO): 8.80 (2H, dd), 8.72 (4H, t), 8.59 (2H, s), 7.92 (4H, m), 7.70 (4H, dd), 7.43 (6H, m), 7.07 (2H, m), 6.75 (2H, d).

[Ru(bq)$_2$(dcbH$_2$)](PF$_6$)$_2$. $[Ru(bq)_2(Cl)_2]$ (150 g, 0.21 mmol) was added to argon-purged DMF (12 mL) and refluxed under argon for 2 h. After cooling to room temperature, the reaction solution was treated with dcb^{2-} (200 mg, 0.62 mmol) dissolved in 12 mL of argon-purged H_2O, and the solution was refluxed again for 18 h. The solution was filtered to remove a green precipitate, and the dark red filtrate was treated with 0.4 M HPF_6 (aq, 1 mL) giving a red-brown precipitate that was filtered and washed with H_2O followed by ether. ^{1}H NMR δ (CD_3CN): 8.98 (4H, q), 8.81 (2H, d), 8.46 (2H, d), 8.25 (2H, s), 8.12 (2H, d), 8.06 (2H, d), 7.81 (4H, m), 7.50 (2H, m), 7.31 (4H, m), 7.04 (4H, m), 6.90 (2H, m).

Characterization. ^{1}H NMR spectra were obtained on a Bruker 300 Hz AMX FT-NMR spectrometer. Attenuated Total Reflectance (ATR) measurements were obtained using a Golden Gate Single Reflection Diamond ATR apparatus on a Nexus 670 Thermo-Nicolet FT-IR and taking 128−256 scans at 4 cm^{-1} resolution. For TiO_2 samples, the background was taken using either a blank TiO_2/glass or TiO_2/FTO slide. Elemental analysis was performed by Atlantic Microlabs, Inc. X-ray crystallography was performed by Arnold Rheingold and co-workers at the University of Delaware. Matrix Assisted Laser Desorption Ionization Mass Spectrometry (MALDI-MS) measurements were performed on a Kratos MALDI-TOF model SEQ mass spectrometer using α-cyano-4-hydroxycinnamic acid as the matrix. Fast Atom Bombardment Mass Spectrometry (FAB-MS) measurements were obtained on a VG70S mass spectrometer; samples were suspended in a *p*-nitrobenzyl alcohol matrix.

MO$_2$ Preparations. Transparent films of colloidal TiO_2 or ZrO_2 nanoparticles were prepared by a previously described sol−gel procedure.[27,28] Sensitizer binding was carried out by placing a MO_2 film in an approximately millimolar sensitizer acetonitrile solution for ~24 h.

Photoluminescence. Corrected photoluminescence (PL) spectra were obtained with a Spex Fluorolog that had been calibrated with a standard tungsten−halogen lamp using procedures provided by the manufacturer. Sensitized films were placed diagonally in a 1 cm square quartz cuvette, immersed in acetonitrile, and purged with nitrogen for at least 15 min. The excitation beam was directed 45° to the film surface, and the emitted light was monitored from the front face of the surface-bound sample and from the right angle in the case of fluid solutions. Photoluminescence quantum yield measurements were performed using the optically dilute technique[29] with $Ru(bpy)_3(PF_6)_2$ in acetonitrile as the actinometer and calculated by eq 1:

$$\phi_{PL} = (A_r/A_s)(I_s/I_r)(n_s/n_r)^2\phi_r \quad (1)$$

where A_r and A_s are the absorbances of the actinometer and sample, respectively, I_r and I_s are the integrated photoluminescence of the actinometer and sample, respectively, n_r and n_s are the refractive indexes of the actinometer and sample solvents, respectively, and ϕ_r is the quantum yield for $Ru(bpy)_3(PF_6)_2$ in acetonitrile ($\phi_r = 0.062$). For lithium titration experiments, 0.1 M $LiClO_4$ in CH_3CN was added via syringe to the cuvette that was continuously purged with nitrogen.

Time-resolved photoluminescence decays were acquired on a nitrogen-pumped dye laser (460 nm) apparatus that has been previously described.[30] For solution studies, the samples were optically dilute ($A \approx 0.1$ at λ_{max}), and the kinetic traces were fit to a first-order kinetic model. For TiO_2 and ZrO_2 studies, the time-resolved photoluminescence decays were fit to a parallel first- and second-order kinetic model, eq 2,

$$PLI(t) = B\left(\frac{k_1 \exp(-k_1 t)}{k_1 + p - p\exp(-k_1 t)}\right) \quad (2)$$

where k_1 is a first-order rate constant analogous to the solution and B is a constant.[31] The parameter p is the product of the observed second-order rate constant, k_2, and the initial concentration of ruthenium excited states, $[Ru^{2+*}]_{t=0}$. For studies involving the sensitizers on TiO_2 or ZrO_2, the excitation beam was directed 45° to the film surface, and the emitted light was collected at 90°.

Electrochemistry. Cyclic voltammetry was performed in 0.1 M tetrabutylammonium hexafluorophosphate ($TBAPF_6/CH_3CN$) electrolyte

(26) von Zelewsky, A.; Gremaud, G. *Helvetica Chimica Acta* **1988**, *71*, 1108.

(27) (a) O'Regan, B.; Moser, J.; Anderson, M.; Grätzel, M. *J. Phys. Chem.* **1990**, *94*, 8720. (b) Barbe, C. J.; Arendse, F.; Comte, P.; Jirousek, M.; Lenzmann, F.; Shklover, V.; Grätzel, M. *J. Am. Ceram. Soc.* **1997**, *80*, 3157. (c) Heimer, T. A.; D'Arcangelis, S. T.; Farzad, F.; Stipkala, J. M.; Meyer, G. J. *Inorg. Chem.* **1996**, *35*, 5319.

(28) Qu, P.; Meyer, G. J. *Langmuir* **2001**, *17*, 6720 and references therein.

(29) Demas, J. N.; Crosby, G. A. *J. Phys. Chem.* **1971**, *75*, 991.

(30) Castellano, F. N.; Heimer, T. A.; Tandhasetti, T.; Meyer, G. J. *Chem. Mater.* **1994**, *6*, 1041.

(31) (a) Kelly, C. A.; Farzad, F.; Thompson, D. W.; Meyer, G. J. *Langmuir* **1999**, *15*, 731. (b) Higgens, G. T.; Bergeron, B. V.; Hasselmann, G. M.; Farzad, F.; Meyer, G. J. *J. Phys. Chem. B* **2006**, *110*, 2598.

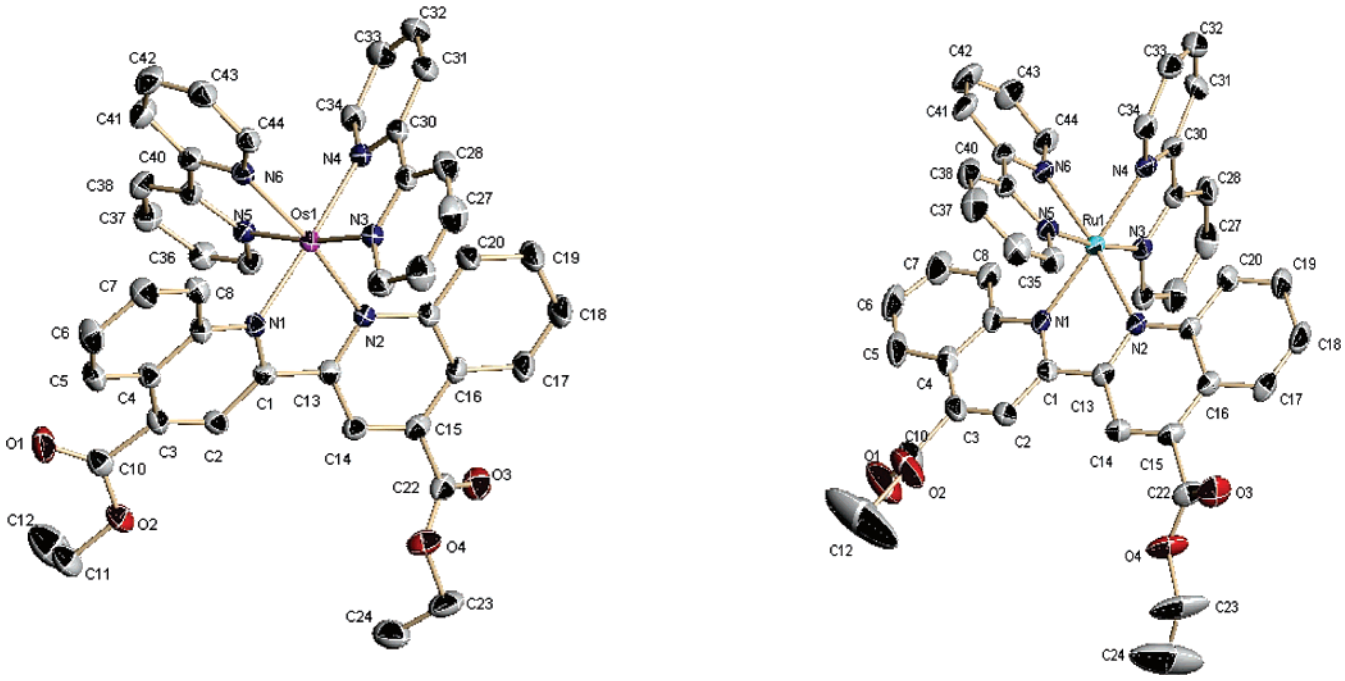

Figure 1. X-ray crystal structures of (a) $[Os(bpy)_2(deebq)](PF_6)_2$ and (b) $[Ru(bpy)_2(deebq)](PF_6)_2$.

with a sensitizer concentration of ~1 mM. A BAS model CV-50W potentiostat was used in a standard three-electrode arrangement with a glassy carbon working electrode, a Pt gauze counter electrode, and Ag/AgCl as the reference electrode. Cyclic voltammetry of the sensitizers bound to TiO_2 was performed in a similar manner with the sensitizer/TiO_2 films deposited on FTO glass as the working electrodes submerged in 0.1 M tetrabutylammonium perchlorate ($TBAClO_4$) acetonitrile. The CV experiments were carried out at room temperature under argon.

Spectroelectrochemistry. Spectroelectrochemistry of derivatized TiO_2 electrodes was performed in a three-electrode custom designed long cuvette cell with a sensitizer/TiO_2/FTO film as the working electrode, a Pt gauze as the counter electrode, and a Ag/AgCl reference electrode, all submerged in 0.1 M $TBAClO_4/CH_3CN$ under a nitrogen atmosphere. Oxidative spectroelectrochemistry was performed on derivatized TiO_2 electrodes by stepping the potential from 1.2 to 1.65 V in the presence of $\sim 10^{-5}$ M redox mediator. The redox mediator utilized depended on the sensitizer being studied. For $[Os(bpy)_2(dcbq)]^{2+}$/TiO_2, the redox mediator was $[Ru(bpy)_3](PF_6)_2$. For the remainder of the sensitizers, the redox mediator was the solvated version of the sensitizer. Comparison of $E_{1/2}(M^{III/II})$ of the sensitizers in solution and on TiO_2 shows that the adsorbed complex has a slightly more negative $E_{1/2}(Ru^{III/II})$, allowing for the intended diffusional redox mediation. For $[Ru(bpy)(deebq)(NCS)_2]$, the oxidation was irreversible, precluding spectral determination of $A(\lambda)$ for Ru^{III}.[20] For all oxidative spectroelectrochemical experiments, the absorbance spectrum of the solvated redox mediator was subtracted from the resulting spectrum of the oxidized sensitizer. Reductive chronoabsorptometry measurements were performed by stepping the potential from 0 V to a negative potential and monitoring UV−vis spectral changes. Desorption during the course of the experiment was found to be negligible.

Absorbance Measurements. UV−vis absorbance measurements were made on a Hewlett-Packard 8453 diode array spectrophotometer. Nanosecond transient absorption measurements were acquired with 532 nm laser excitation (ca. 8 ns fwhm from a Nd:YAG Continuum Surelite II laser), 417 nm (H_2 Raman shifter with 355 nm laser light), or 683 nm (H_2 Raman shifter with 532 nm laser light). The sample was protected from a pulsed 150 W Xe probe beam using a fast shutter and appropriate UV and heat absorbing glass and solution filter combinations. Each kinetic trace was acquired averaging 60−100 laser shots. Samples were nitrogen purged for at least 15 min prior to transient absorption studies.

Comparative actinometry was carried out with $[Ru(bpy)_3](PF_6)_2$ doped into a PMMA thin film deposited on a glass microscope slide as the actinometer.[32] The extinction coefficient difference between the excited-state and ground-state has been previously reported to be $(-1.00 \pm 0.09) \times 10^4\ M^{-1}\ cm^{-1}$ at 450 nm, with an excited-state quantum yield of unity.[32] Extinction coefficients for the reduced and oxidized compounds were obtained from spectroelectrochemical measurements.

Resonance Raman. Spectra were collected using a Spex 14018 double monochromator equipped with a Spex Compudrive controller and a Hamamatsu R943-02 photomultiplier (PMT) cooled by a Products for Research thermoelectric liquid heat exchanged housing. The PMT signal was processed with a Hamamatsu C3866 discriminator/amplifier and counted with a computer interfaced Philips PM 6680 counter. LabView was used for data acquisition and monochromator control. Excitation at 406.7, 413.1, 415.4, 468.0, 476.2, 482.5, 520.8, 530.9, and 568.2 nm was provided by a Coherent Innova Sabre Kr^+ laser. Plasma lines were eliminated with a grating. The laser beam was focused on the sample (in a melting point tube) and maintained at 50 ± 5 mW. Scattered light was collected at 45° from the excitation using a conventional two-lens collection system. Spectra were acquired at 1 cm^{-1} steps and with a 10 s integration time.

Results

Crystals of $[Ru(bpy)_2(deebq)](PF_6)_2$ and $[Os(bpy)_2(deebq)](PF_6)_2$ suitable for X-ray diffraction studies were isolated, Figure 1. Both crystals were monoclinic and of the same space group, $P2(1)/c$.

The unit cell lengths for the compounds were quite different, with the largest disparity occurring along the axis a, Table 1. In addition, there was a significant difference in the β angles, 96.5° for $[Ru(bpy)_2(deebq)](PF_6)_2$ and 112.9° for $[Os(bpy)_2(deebq)](PF_6)_2$, as well as the deebq dihedral angles, 16.5° and 25.2°, respectively.

Absorption spectra for $[Ru(bpy)_2(deebq)](PF_6)_2$ and $[Os(bpy)_2(deebq)](PF_6)_2$ in acetonitrile are provided in Figure 2.

(32) Bergeron, B.; Kelly, C. A.; Meyer, G. J. *Langmuir* **2003**, *19*, 8389.

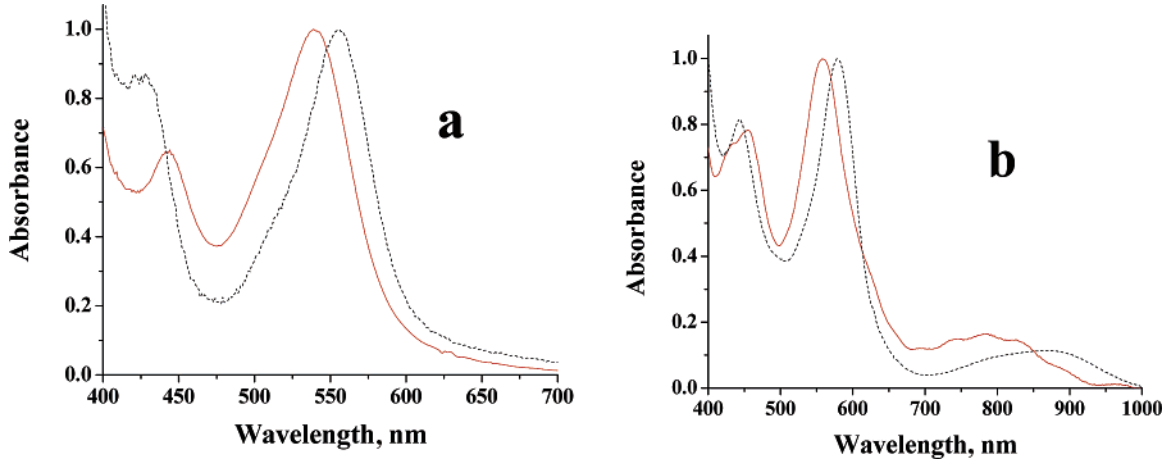

Figure 2. Normalized absorbance spectra of (a) $[Ru(bpy)_2(deebq)](PF_6)_2$ and (b) $[Os(bpy)_2(deebq)](PF_6)_2$ in neat acetonitrile (dashed line) and anchored to TiO_2 (solid line).

Table 1. Crystal Data and Structure Refinement for $[Ru(bpy)_2(deebq)](PF_6)_2$ and $[Os(bpy)_2(deebq)](PF_6)_2$

	$[Ru(bpy)_2(deebq)](PF_6)_2$	$[Os(bpy)_2(deebq)](PF_6)_2$
formula	$C_{47}H_{42}F_{12}N_6O_5P_2Ru$	$C_{47}H_{42}F_{12}N_6O_5P_2Os$
fw	1161.88	1251.01
crystal system	monoclinic	monoclinic
space group	*P*2(1)/*c*	*P*2(1)/*c*
a, Å	17.5217(14)	19.0259(11)
b, Å	14.1894(11)	13.9453(8)
c, Å	18.7241(15)	19.2470(12)
β, deg	96.4570(10)	112.8890(10)
biq dihedral angle, deg	16.5	25.2
V, Å^3	4625.7(6)	4704.6(5)
Z	4	4
cryst color	deep red	black
crystal dimensions, mm^3	0.2 × 0.2 × 0.2	0.35 × 0.25 × 0.2
D(calcd), g cm^{-3}	1.668	1.766
μ(Mo Kα), cm^{-1}	5.12	2.88
temp, K	173(2)	173(2)
diffractometer	Siemens P4/CCD	Siemens P4/CCD
radiation	Mo Kα (λ = 0.710 73 Å)	Mo Kα (λ = 0.710 73 Å)
R(*F*), %	7.80	3.74
$R(wF^2)$,[a] %	20.17	11.69

[a] Quantity minimized = $R(wF^2) = \sum [w (F_o^2 - F_c^2)^2]/\sum [(wF_o^2)_2]^{1/2}$; R = $\sum \Delta/\sum (F_o)$, $\Delta = |(F_o - F_c)|$.

Two broad metal-to-ligand charge transfer (MLCT) absorption bands were observed in the visible region, the higher energy band is assigned as Ru → bpy charge transfer and the lower energy band as Ru → deebq. For $[Ru(bq)_2(deeb)](PF_6)_2$ and $[Ru(deebq)_2(bpy)](PF_6)_2$, the higher energy M → deeb/bpy band exists as a lower intensity shoulder to the M → bq/deebq charge-transfer absorption band. For $[Os(bpy)_2(deebq)](PF_6)_2$, an additional band in the near-IR was assigned to a direct singlet-to-triplet transition.[33] The absorbance spectra of the carboxylic acid and carboxylate forms of the compounds were measured in methanol. The carboxylic acid derivatives displayed absorption features that were very similar to that of the ethyl ester compounds in acetonitrile. Deprotonation of the carboxylic acid groups lead to a significant blue shift of the M → bq′ charge-transfer band and a smaller red shift of the M → bpy band. The singlet-to-triplet absorption band of $[Os(bpy)_2(dcbq)]$ also blue shifted significantly upon deprotonation of the carboxylic acid groups. These spectral properties compare well with previously reported results for similar heteroleptic compounds.[34,35]

All five compounds were found to bind to nanocrystalline TiO_2 films with a limiting surface coverage, Γ_o, of ~8.0×10^{-8} mol/cm^2. Small but reproducible spectral shifts were observed upon binding to the nanocrystalline thin films. The absorption spectra of the surface bound compounds most closely resembled the carboxylate forms of the sensitizers measured in methanol, Figure 2. We abbreviate the carboxylate forms of the ligands as dcb or dcbq.

The $[Ru(bpy)_2(deebq)](PF_6)_2$, $[Ru(bq)_2(deeb)](PF_6)_2$, and $[Ru(deebq)_2(bpy)](PF_6)_2$ compounds displayed room temperature photoluminescence (PL) in acetonitrile solution, while no PL was observed from $[Os(bpy)_2(deebq)](PF_6)_2$ and $[Ru(bpy)(deebq)(NCS)_2]$ from 500 to 800 nm under the same conditions. Excited-state decay followed a first-order kinetic model, and the extracted lifetimes, τ, are listed in Table 2. Excited-state decay of the sensitizers anchored to ZrO_2 or TiO_2 were nonexponential and were well described by a parallel first- and second-order kinetic model.[31]

The corrected PL spectra were used to estimate the Gibbs free energy stored in the thermally equilibrated MLCT excited state. An attempt was made to accomplish this with a single mode Franck−Condon line shape analysis as has been previously described.[36] However, the PL was observed at such low energy that a meaningful fit could not be obtained even at 77 K. We therefore utilized the more traditional approach of a tangent line drawn on the high-energy side of the corrected room temperature spectra.[38] The reduction potentials of the thermally equilibrated luminescent excited state were then calculated from eq 3 as previously described.[39]

$$E_{1/2}(Ru^{III/II*}) = E_{1/2}(Ru^{III/II}) - \Delta G_{es} \qquad (3)$$

Attenuated total reflectance FTIR spectroscopy was used to characterize the compounds in the solid state and when anchored to TiO_2. An intense band at 1713 cm^{-1} assigned to the

(33) Kober, E.; Meyer, T. J. *Inorg. Chem.* **1982**, *21*, 1324.
(34) Nazeeruddin, Md. K.; Zakeeruddin, S. M.; Humphry-Baker, M. J.; Liska, P.; Vlachopoulos, V. S.; Fischer, C.-H.; Grätzel, M. *Inorg. Chem.* **1999**, *38*, 6298.
(35) Qu, P.; Meyer, G. J. *Langmuir* **2001**, *17*, 6720.
(36) Casper, J. V.; Meyer, T. J. *J. Am. Chem. Soc.* **1983**, *105*, 5583.
(37) Kober, E. M.; Caspar, J. V.; Lumpkin, R. S.; Meyer, T. J. *J. Phys. Chem.* **1986**, *90*, 3722.
(38) Arnold, D. R.; Baird, N. C.; Bolton, J. R.; Brand, J. C. D.; Jacobs, P. W. M.; DeMayo, P.; Ware, W. R. *Photochemistry. An Introduction*; Academic Press: New York and London, 1974; p 13.
(39) Rehm, D.; Weller, A. *Isr. J. Chem.* **1970**, *8*, 259.

Table 2. Photophysical and Electrochemical Properties of Sensitizers and TiO_2 Bound Sensitizers in Acetonitrile[a]

sensitizer	λ_{abs}, nm (ϵ, M^{-1} cm^{-1})[b] Ru → bpy′ II Ru → bq′	λ_{PL},[c] nm	τ, ns	$E_{1/2}(M^{III/II})$,[d] V	$E_{1/2}(M^{2+/+})$,[d] V	$E_{1/2}(M^{III/II*})$,[d] V	ΔG_{es},[e] eV	ϕ_{PL} $\times 10^{-3}$
$[Ru(bpy)_2(deebq)](PF_6)_2$	427 (6.4×10^3), 555 (7.4×10^3)	835	90	1.45	−0.60	−0.20	1.64	1.9
$[Ru(bpy)_2(dcbq)]/TiO_2$	444, 539	800	430	1.39	−0.70	−0.38	1.77	
$[Os(bpy)_2(deebq)](PF_6)_2$	442 (7.7×10^3), 579 (9.5×10^3)	*f*	11	1.05	−0.59	*f*	*f*	*f*
$[Os(bpy)_2(dcbq)]/TiO_2$	451, 565		20	0.98	−0.70			
$[Ru(bq)_2(deeb)](PF_6)_2$	488 (7.1×10^3), 530 (9.8×10^3)	728	210	1.52	−0.79	−0.33	1.85	5.3
$[Ru(bq)_2(dcb)]/TiO_2$	491, 542	775	400	1.44	−0.90	−0.33	1.77	
$[Ru(bpy)(deebq)_2](PF_6)_2$	490 (6.0×10^3), 573 (1.3×10^4)	780	590	1.55	−0.56	−0.15	1.70	16
$[Ru(bpy)(dcbq)_2]/TiO_2$	500, 573	800	780	1.50	−0.65	−0.20	1.70	
$[Ru(bpy)(deebq)(NCS)_2]$	450 (1.1×10^4), 626 (1.2×10^4)	*f*	10	0.86	−0.84	*f*	*f*	*f*
$[Ru(bpy)(dcbq)(NCS)_2]/TiO_2$	432, 593		15	0.72	−0.95			

[a] All measurements were performed at room temperature. [b] Absorption maxima of the visible MLCT bands. [c] Corrected photoluminescence maxima, ±5 nm. [d] Half-wave potentials measured by cyclic voltammetry in 0.1 M $TBAPF_6$ acetonitrile electrolyte versus the standard calomel electrode, SCE. The abbreviation $M^{III/II}$ represents the metal-based reductions, $M^{2+/+}$ represents the first ligand-based reductions, and $M^{III/II*}$ is the excited-state reduction potential. [e] The Gibbs free energy stored in the thermally equilibrated excited state. [f] A room-temperature emission maximum could not be observed with $\lambda < 850$ nm that precludes analysis of excited-state reduction potentials, photoluminescent quantum yields, and the free energy stored in the excited state.

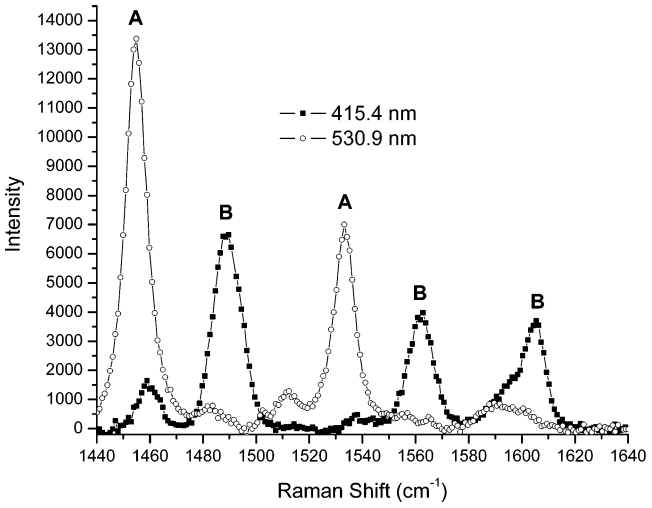

Figure 3. Resonance Raman spectra of $[Ru(bpy)_2(deebq)](PF_6)_2$ in acetonitrile-d_6 at the indicated excitation wavelengths. Letters **A** and **B** denote deebq and bpy vibrational modes, respectively.

asymmetric C═O stretch was observed for the ester derivatives, while the carboxylate forms showed two bands at 1597 and 1387 cm^{-1}.[40,41] Interestingly, when either the ester or the carboxylate forms were anchored to TiO_2, their FTIR spectra were virtually superimposable showing intense bands at approximately the same energies as the carboxylate compound. The only exception to this was $[Ru(bpy)(deebq)_2](PF_6)_2$, which showed some absorbance at ~1713 cm^{-1} characteristic of unhydrolyzed ethyl esters after surface attachment. Consistent with previous results, the FTIR data indicated that the carboxylate form of the compounds were present on the ZrO_2 or TiO_2 surfaces.[28]

Shown in Figure 3 is resonance Raman spectra of $[Ru(bpy)_2(deebq)](PF_6)_2$ in acetonitrile collected at different excitation wavelengths. The bipyrdine and biquinoline vibrational modes enhanced were readily assigned based on previous publications.[42,43] The biquinoline modes were selectively enhanced with long wavelength excitation (530.9 or 568.2 nm) of $[Ru(bpy)_2(deebq)]^{2+}$. As the excitation energy increased, contributions from the bpy′ modes became more apparent. With 415.4 nm excitation, most of the enhancement was from bpy with only a small contribution from biquinoline.

All the compounds except $[Ru(bpy)(deebq)(NCS)_2]$ displayed quasi-reversible $M^{III/II}$ waves in cyclic voltammetery measurements in acetonitrile electrolyte with scan rates from 10 to 500 mV/s. The redox processes were classified as quasi-reversible because the anodic and cathodic currents were approximately equal but the peak-to-peak separation was greater than 80 mV.[44] The $M^{III/II}$ reduction potential for $[Os(bpy)_2(deebq)]^{2+}$ was 400 mV more negative than that of $[Ru(bpy)_2(deebq)]^{2+}$, Table 1. As the number of bq ligands increased in the heteroleptic Ru(II) compounds, $E_{1/2}(Ru^{III/II})$ became increasingly more positive. Quasi-reversible waves at ~ −0.7 V vs SCE were assigned to the first ligand-based reductions, $E_{1/2}(M^{2+/+})$. The reductions were about 200 mV more positive when ethyl ester groups replaced hydrogen atoms in the 4 and 4′ positions of the diimine ligand. Comparative studies show that deebq is the most easily reduced followed by bq, deeb, and bpy. The electrochemical data are consistent with previous reports for related compounds.[26]

Cyclic voltammetry performed on sensitized TiO_2 films also showed quasi-reversible waves in acetonitrile electrolyte. The $E_{1/2}(M^{III/II})$ potentials were slightly more negative (~80 mV) when compared to data obtained in the electrolyte solution. The $E_{1/2}(M^{2+/+})$ ligand-based reductions were consistently 100 mV more negative on the surface than that measured in the electrolyte solution. These data are summarized in Table 2.

The $Ru^{III/II}$ wave for $[Ru(bpy)(deebq)(NCS)_2]$ was quasi-reversible at faster scan rates but became irreversible at slower scan rates. The oxidative process was 82% reversible at 50 mV/s and completely reversible at 500 mV/s, consistent with an ~1 s lifetime of the oxidized compound. The oxidized N3 sensitizer, $[Ru^{III}(dcb)_2(NCS)_2]^+$, also has a lifetime of 0.1−1 s in CH_3CN.[45] The estimated $E_{1/2}(Ru^{III/II})$ for $[Ru(bpy)(deebq)(NCS)_2]$ is similar to that reported for N3, Table 1.

Spectroelectrochemistry was used to obtain the absorption spectra of the reduced and oxidized forms of the compounds anchored to the TiO_2 surface. Application of a potential more negative than that of the first ligand-based reduction for samples

(40) Finnie, K. S.; Bartlett, J. R.; Woolfrey, J. L. *Langmuir* **1988**, *14*, 2744.
(41) Dobson, K.; McQuillan, A. *Spectrochim. Acta, Part A* **2000**, *5*, 557.
(42) Tait, C. D.; MacQeen, D. B.; Donahue, R. J.; DeArmond, M. K.; Hanck, K. W.; Wertz, D. W. *J. Phys. Chem.* **1986**, *90*, 1766.
(43) Chowdhury, J.; Ghosh, M.; Misra, T. N. *Spectrochim. Acta, Part A* **2000**, *56*, 2107.
(44) Bard, A. J.; Faulkner, L. R. *Electrochemical Methods: Fundamentals and Applications*, 2nd ed.; John Wiley & Sons: New York, 2001.
(45) (a) Moser, J. E.; Noukakis, U. B.; Tachibana, Y.; Klug, D. R.; Durrant, J. R.; Humphrey-Baker, R.; Grätzel, M. *J. Phys. Chem. B* **1998**, *102*, 3649. (b) Das, S.; Kamat, P. V. *J. Phys. Chem. B* **1998**, *102*, 8954.

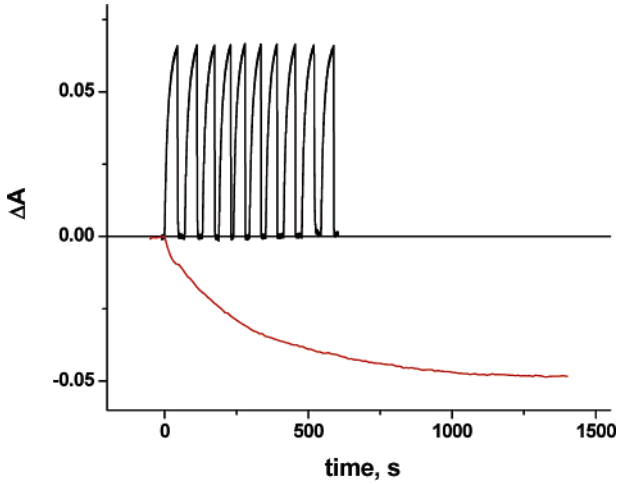

Figure 4. Absorption changes observed after electrochemical reduction and oxidation of $[Ru(bpy)_2(dcbq)]/TiO_2$ in acetonitrile electrolyte. The positive absorption changes correspond to $[Ru(bpy)_2(dcbq)]/TiO_2$ reduction monitored at 470 nm (upper black traces) and induced by cycling the potential between 0.0 and −0.75 V vs SCE. The oxidation of $[Ru(bpy)_2(dcbq)]/TiO_2$ (lower red trace) was observed at 550 nm after stepping the potential from 1.10 V to +1.60 V vs SCE.

results in visible absorbance changes. The spectral changes were consistent with formation of the reduced compound on TiO_2. The same spectra could be observed upon steady-state photolysis (514.5 nm) of the sensitized TiO_2 films in 0.5 M triethylamine/CH_3CN. The application of a potential more positive than the $M^{III/II}$ potential resulted in the appearance of the oxidized compound on TiO_2. The time scale for the oxidation was much longer than that for reduction, and the solvated version of the sensitizer was often used to mediate oxidation.

Chronoabsorption measurements were made to obtain the apparent diffusion coefficients, D_{app}, for intermolecular hole and electron hopping at saturation surface coverages across the nanocrystalline TiO_2 surfaces.[46−48] For all the sensitizers, it took at least 10 times as long to oxidize the surface bound sensitizers as it did to reduce them. Figure 4 shows typical data that demonstrates that the sensitizers could be reversibly reduced and reoxidized in about a minute, while oxidation was incomplete after 20 min. These redox processes occurred with retention of isosbestic points. Occasionally, some sensitizer desorption was observed particularly during the sluggish oxidation.

About 60% of Anson plots, ΔA versus $t^{1/2}$, were found to be linear, and the apparent diffusion constant, D_{app}, was abstracted from these data as previously described.[48] For reduction of $Ru(bpy)_2(dcbq)/TiO_2$ in acetonitrile electrolyte, a $D_{app}(Ru^{2+/+}) = (3.3 \pm 0.3) \times 10^{-12}$ m^2/s was obtained from absorption changes observed after stepping the applied potential from 0.00 V to −0.75 V vs SCE, while $D_{app}(Ru^{III/II})$ was obtained similarly by stepping the applied potential from 1.10 V to +1.60 V, $D_{app}(Ru^{III/II}) = (2 \pm 1) \times 10^{-13}$ m^2/s.

Nanosecond transient absorption spectra of the sensitizers were obtained in acetonitrile and when anchored to TiO_2 and ZrO_2 thin films, Figure 5. The absorption difference spectra of the sensitizers measured in acetonitrile and anchored to ZrO_2 were within the same experimental error and were assigned to the MLCT excited state. The difference spectra showed positive ΔA features below ~425 nm and beyond ~600 nm, as well as a bleach of the ground-state absorption from ~500−600 nm. Excited-state decay was exponential in fluid solution and required a parallel first- and second-order kinetic model for excited states anchored to ZrO_2.[31] In all cases, the kinetic rate constants abstracted agreed well with those obtained by time-resolved photoluminescence measurements. UV−visible absorption spectra recorded before and after transient absorption studies of the mono-biquinoline compounds showed no evidence for photochemistry. For $[Ru(bq)_2(deeb)](PF_6)_2$ and $[Ru(bpy)(deebq)_2](PF_6)_2$ photochemical products were observed after photolysis even at low irradiances. In agreement with the results of von Zelewsky and Gremaud, the biquinoline ligand was found to be photolabile.[26] For example, laser excitation of $[Ru(deebq)_2(bpy)]^{2+}$ in acetonitrile yielded *cis*-$[Ru(bpy)(deebq)(CH_3CN)_2]^{2+}$ that was isolated and characterized by ^{1}H NMR. This photoproduct was successfully used as a precursor in the synthesis of $[Ru(bpy)(deebq)(NCS)_2]$.

Nanosecond transient absorption spectra of the sensitizers anchored to TiO_2 showed the presence of the MLCT excited state and an additional product that had a lifetime several orders of magnitude greater. No corresponding long-lived state was observed by time-resolved PL measurements. The absorption difference spectrum of the long-lived component was simulated by standard addition of the visible absorption spectrum of the reduced and oxidized forms of the compound minus two ground-state spectra, $\Delta A = A(M^{III}) + A(M^{+}) - 2A(M^{II})$. The simulations were in excellent agreement with the observed difference spectra for the long-lived component, Figure 5b inset right-hand side. This charge separated state was easily distinguished from the more common interfacial charge separated state with an oxidized sensitizer and a conduction band electron, Figure 5b inset left-hand side. The positive absorptions observed at ~500 and 700 nm are characteristic of the reduced sensitizers.

The long-lived component returned cleanly to ground-state products on a millisecond time scale. Transients recorded at probe wavelengths that provided the best signal-to-noise were well described by the Kohlrausch−Williams−Watts (KWW) model, Figure 6 and eq 4,

$$I(t) = \alpha \exp - (kt)^{\beta} \qquad 0 < \beta < 1 \tag{4}$$

where k is the maximum rate constant in a distribution of rate constants α is the initial amplitude, and β is inversely related to the width of this underlying distribution.[27c] Kinetic fits to a large number of samples gave $k = (8 \pm 5) \times 10^5$ s^{-1} and $\beta = 0.25 \pm 0.05$.

Comparative actinometry was used to determine quantum yields for formation of the charge-separated states. The yields were found to be independent of the excitation irradiance and only weakly dependent on the sensitizer surface coverage.[49] A notable wavelength dependence was observed, Table 3. Significant charge separation was also observed for $Ru(bpy)(dcbq)(NCS)_2/TiO_2$; however the extinction coefficients were unknown, due to the reactivity of the oxidized sensitizer, so that absolute yields could not be quantified. Also given in Table 2 are the reduction potentials of the initially formed Franck−Condon excited state, eq 5,

$$E°(M^{III/II**}) = E_{1/2}(M^{III/II}) - E_{op} \tag{5}$$

(46) Bonhote, P.; Gogniat, E.; Tingry, S.; Barbe, C.; Vlachopoulos, N.; Lenzmann, F.; Comte, P.; Grätzel, M. *J. Phys. Chem. B* **1998**, *102*, 1498.
(47) Trammel, S. A.; Meyer, T. J. *J. Phys. Chem. B* **1999**, *103*, 104.
(48) Anson, F. C.; Blauch, D. N.; Saveant, J.-M.; Shu, C.-F. *J. Am. Chem. Soc.* **1991**, *113*, 1922.

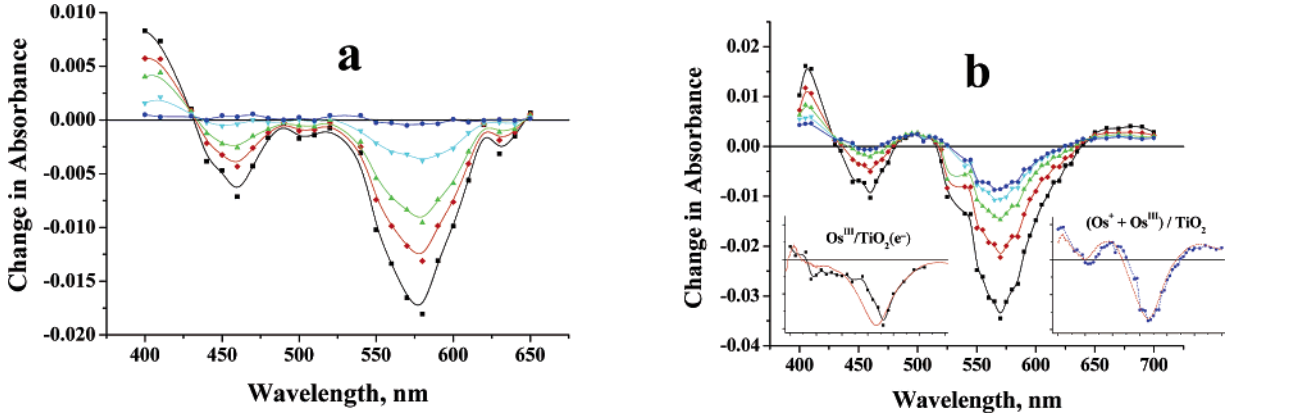

Figure 5. Transient absorbance spectra of (a) $[Os(bpy)_2(dcbq)]/ZrO_2$ and (b) $[Os(bpy)_2(dcbq)]/TiO_2$ following 417 nm light excitation (3.5 mJ/cm^2, 8 ns fwhm). The delay times for the ZrO_2 sample were as follows: 5 ns (black line, ■), 10 ns (red line, ♦), 15 ns (green line, ▲), 30 ns (cyan line, ▼), and 100 ns (blue line, ●). The delay times for the TiO_2 sample were as follows: 10 ns (black line, ■), 25 ns (red line, ♦), 100 ns (green line, ▲), 500 ns (cyan line, ▼), and 2 μs (blue line, ●). The inset shows a simulation over the same spectral range of the simulated spectra (dashed) overlaid with the experimental data obtained 5 μs after pulsed excitation of $[Os(bpy)_2(dcbq)]/TiO_2$ in 0.1 M $LiClO_4$ acetonitrile (left-hand side) and in neat acetonitrile (right-hand side).

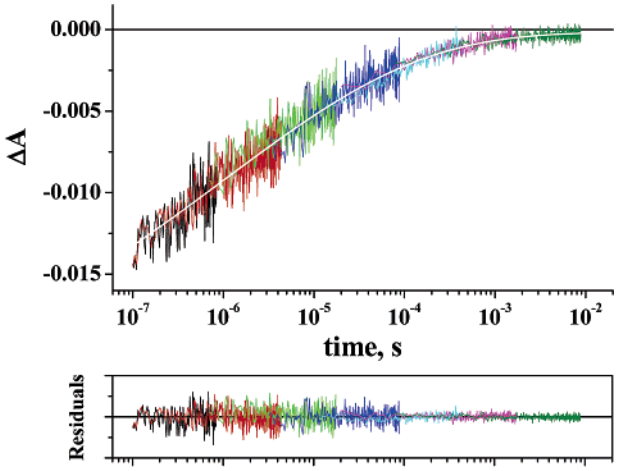

Figure 6. Absorption change monitored at 570 nm following 417 nm laser light excitation (~3.5 mJ/cm^2, 8 ns fwhm) of $[Os(bpy)_2(dcbq)]/TiO_2$ ($\Gamma = 6.5 \times 10^{-8}$ mol/cm^2). Overlaid on the data is a best fit (white line) to the Kohlrausch−Williams−Watts model. Residuals for the fit are also shown.

Table 3. Excitation Wavelength Dependent Quantum Yields[a]

sensitizer	417 nm ($E°(M^{III/II*})$)[b]	532 nm ($E°(M^{III/II*})$)[b]	683 nm ($E°(M^{III/II*})$)[b]
$[Ru(bpy)_2(dcbq)]/TiO_2$	0.17 ± 0.02 (−1.59)	0.05 ± 0.02 (−0.95)	*c*
$[Os(bpy)_2(dcbq)]/TiO_2$	0.18 ± 0.02 (−2.00)	0.08 ± 0.02 (−1.36)	0.05 ± 0.01 (−0.84)
$[Ru(bq)_2(dcb)]/TiO_2$	0.06 ± 0.02 (−1.54)	≤0.02 (−0.90)	*c*
$[Ru(bpy)(dcbq)_2]/TiO_2$	0.04 ± 0.02 (−1.48)	≤0.02 (−0.84)	*c*

[a] All measurements performed in acetonitrile at room temperature. [b] The reduction potential of the initially formed Franck−Condon excited state, calculated by eq 5. [c] Sensitizer did not appreciably absorb light at this wavelength.

where E_{op} is the excitation energy.[40] The addition of less than ~1 mM concentrations of $LiClO_4$ to the external acetonitrile was found to increase the charge separation yields by about 10−20% with 417 nm light excitation. When higher Li^+ concentrations were employed, difference spectra consistent with an oxidized sensitizer and an injected electron, $M^{III}/TiO_2(e^-)$, were observed, Figure 5b inset left-hand side.[49] For $[Ru(bpy)_2(dcbq)]/TiO_2$ quenching of the steady-state photoluminescence was observed at >20 mM Li^+ concentrations.

(49) Hoertz, P. G. Thesis Johns Hopkins University, 2003.

Discussion

Ultrafast electron injection at sensitized TiO_2 interfaces, while of debatable importance in regenerative solar cells, has been exploited here to drive photoredox reactions that are thermodynamically uphill in fluid solution. Indeed, control experiments in fluid acetonitrile gave no evidence for excited-state electron transfer. The ability to drive such "uphill" redox reactions and utilize energy that would otherwise be irreversibly lost represents an important step toward the realization of solar conversion efficiencies that exceed the Shockley−Queisser limit.[1,2]

The proposed mechanism for photoinduced TiO_2 mediated charge separation is shown schematically (Scheme 2). Ultrafast electron injection into TiO_2 is followed by rapid reduction (<10 ns) of a surface bound sensitizer. Lateral intermolecular charge transfer across the semiconductor surface ultimately yields ground state products. Thus absorption of a single photon yielded well-defined redox equivalents that typically stored 15−25% more free energy than did the photoluminescent excited state of the sensitizer. For example, the photoinduced charge separation observed after light excitation of $[Ru(bpy)_2(dcbq)]/TiO_2$ can be designated as shown in eq 6.

$$Ru(bpy)_2(dcbq)^{**}/TiO_2 + Ru^{II}(bpy)_2(dcbq)/TiO_2 \rightarrow Ru^{III}(bpy)_2(dcbq)^+/TiO_2 + Ru^{II}(bpy)_2(dcbq^-)^-/TiO_2 \quad (6)$$

The redox equivalents formed store 2.09 eV of free energy, while the luminescent excited state stores only about 1.77 eV. In addition, charge separation lasted for periods of milliseconds, while the excited states decayed on a nanosecond time scale. Below we discuss mechanistic details of the charge separation processes, electron injection and sensitizer reduction as well as lateral intermolecular charge transfer processes that ultimately lead to recombination.

Ultrafast Electron Injection. Subpicosecond electron injection is now well documented at sensitized TiO_2 interfaces.[8−15] The transient data are highly nonexponential and show an excitation wavelength dependence. The origin of the complex

Scheme 2

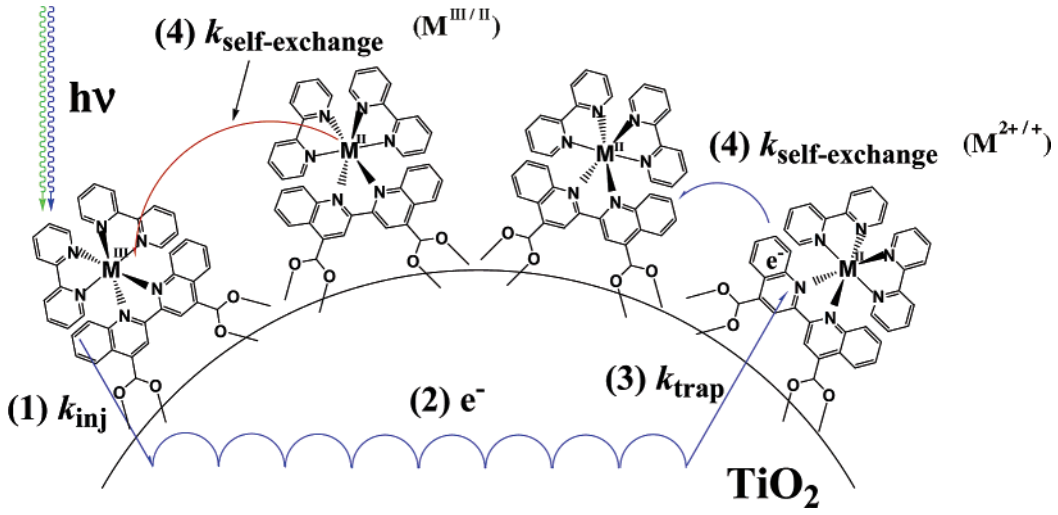

kinetics remains unresolved but may reflect interfacial heterogeneity. Sundstrum has proposed that the singlet state injects electrons in subpicoseconds, while the triplet injects on a slower picosecond time scale.[13] Triplet injection was thought to be particularly important when light excitation promoted an electron to a ligand remote or weakly coupled to the semiconductor surface. Moser and Grätzel have recently shown that the slower picosecond components were essentially absent from sensitized TiO_2 films equilibrated in ionic solutions, behavior attributed to removal of the weakly bound sensitizers.[50]

Under the experimental conditions employed here, the photoluminescent excited state did not inject electrons into TiO_2. Nanosecond time resolution precludes the direct determination of the injection dynamics but were consistent with $k_{inj} > 10^8$ s^{-1}. The excitation wavelength dependent quantum yields were, however, characteristic of injection from vibrationally hot excited states and are not easily explained by other mechanisms.[19,51] To a first approximation, these data can be rationalized based on the reduction potential of the initially formed Franck−Condon excited state, Table 3. The stronger the photoreductant, the higher the injection yield. Injection is thus competitive with vibrational relaxation and/or intersystem crossing of the photoexcited sensitizer. For Ru and Os polypyridyl compounds, this is known to be a subpicosecond process.[55]

Gerischer has stated that the electron transfer rate constants are directly proportional to the overlap of the donor levels of the excited sensitizer $W_{don}(E)$ with the density of unoccupied acceptor levels of the semiconductor $D(E)$,

$$k_{inj} \approx \int \kappa(E)\, D(E)\, W_{don}(E)\, dE \qquad (7)$$

where $\kappa(E)$ is the transfer frequency.[52] There is good reason to believe that the increased injection yields with excitation energy reflect a larger overlap integral in eq 7. Electrochemical measurements indicate that the density of TiO_2 acceptor states increases exponentially in energy.[53] The number of vibrational and electronic states accessible to the photoexcited sensitizer also increases with excitation energy.[55] Therefore, a greater overlap integral is expected for sensitizers excited with blue light relative to green or red light. This conclusion is consistent with recent ultrafast injection measurements[8−15] and with early pioneering photoluminescence studies[54] both of which have provided compelling evidence for faster injection rates as the energy separation between the excited donor and the conduction band edge increases.

A close inspection of the quantum yield data in Table 3 shows some subtle effects that cannot easily be rationalized solely on reduction potentials. Fortunately, variable light excitation studies into the energetically well-resolved charge transfer absorption bands of these heteroleptic sensitizers provided new insights. While some excited state mixing undoubtedly occurs, the resonance Raman, spectroscopic, and electrochemical data indicate that the lower energy absorption band ($\lambda_{max} \approx 550$ nm) is predominately M → bq′ charge transfer, while the higher energy band ($\lambda_{max} \approx 450$ nm) is M → bpy in nature. Therefore, blue light excitation of $[M(bpy)_2(dcbq)]/TiO_2$ promotes an electron to a remote and unbound bpy ligand, $[Ru(bpy^-)(bpy)(dcbq)]^*/TiO_2$ that injects electrons more efficiently than does M→bq′ excitation, $[M(bpy)_2(dcbq^-)]^*/TiO_2$. This must reflect the stronger reducing power of the bpy localized excited state and a larger overlap integral in eq 7. This conclusion challenges the notion that strong electronic coupling through the carboxylate containing ligand and the semiconductor is required for ultrafast electron injection. The Os sensitizer yields were lower than one would expect based on comparisons with the Ru excited-state reduction potentials. As pointed out by McKusker, the heavier Os metal center is expected to increase intersystem crossing dynamics, and this lowers the ultrafast injection yield.[14] We note that light excitation into the singlet-to-triplet absorption band results in a significant injection. Therefore, to the degree that spin effects can be realized with these heavy transition metal

(50) Wenger, B.; Gratzel, M.; Moser, J.-E. *J. Am. Chem. Soc.* **2005**, *127*, 12150.
(51) Liu, F.; Meyer, G. J. *J. Am. Chem. Soc.* **2005**, *127*, 824.
(52) (a) Gerischer, H. *Photochem. Photobiol.* **1972**, *16*, 243. (b) Gerischer, H.; Willig, F. *Top. Curr. Chem.* **1976**, *61*, 31. (c) Gerischer, H. *Pure Appl. Chem.* **1980**, *52*, 2649.
(53) Kay, A.; Humphrey-Baker, R.; Grätzel, M. *J. Phys. Chem.* **1994**, *98*, 952.
(54) (a) Kajiwara, T.; Hasimoto, K.; Kawai, T.; Sakata, T. *J. Phys. Chem.* **1982**, *86*, 4516. (b) Kajiwara, T.; Hasimoto, K.; Kawai, T.; Sakata, T. *J. Phys. Chem.* **1988**, *92*, 4636. (c) Sakata, T.; Hasimoto, K.; Hiramoto, M. *J. Phys. Chem.* **1990**, *94*, 1788.
(55) (a) Damrauer, N. H.; Cerullo, G.; Yeh, A.; Boussie, T. R.; Shank, C. V.; McCusker, J. K. *Science* **1997**, *275*, 54. (b) Bhasikuttan, A. C.; Suzuki, M.; Nakashima, S.; Okada, T. *J. Am. Chem. Soc.* **2002**, *124*, 8398.

compounds, this observation suggests that vibrationally "hot" triplet states can also undergo ultrafast injection processes.[33]

The quantum yields were found to be insensitive to the equilibration time of the sensitized film[50] but could be tuned by the addition of Li^+ cations to the external solution. Lithium cations are known to be "potential determining ions" that adsorb to TiO_2 and shift the conduction band edge positive on an electrochemical scale.[56−58] Lithium concentrations less than about 1 mM were found to increase the injection yields by 10−20%. At higher Li^+ concentrations, only the oxidized sensitizer and the $TiO_2(e^-)$ were observed spectroscopically, presumably because the conduction band edge was below the sensitizer reduction potential (see below for further discussion).

Sensitizer Reduction. Photoinitiated electron transfer from TiO_2 to molecular acceptors has been previously studied.[18] This process represents an unwanted loss mechanism in dye sensitized solar cells, for example. It is known that the electron-transfer rate constants are sensitive to temperature and to thermodynamic driving force in a manner consistent with Marcus theory.[59,60] It is also known that transport of the injected electron in TiO_2 can influence the observed dynamics.[61,62]

In the present study, the molecular acceptors were ground state sensitizers that were photoreduced in less than 10 ns. Electrochemical studies demonstrate that the sensitizers were more easily reduced than the TiO_2 nanoparticles. Furthermore, when the sensitizers were excited with visible light in the presence of a sacrificial electron donor, the reduced forms of the sensitizers were observed. Taken together, these results demonstrate that the first reduction potential of the sensitizers lies below the conduction band edge $E_{cb} < E_{1/2}(M^{2+/+})$.

These energetics enabled us to measure the ligand-based reduction potentials of the sensitizers anchored to TiO_2 for the first time. The sensitizer/TiO_2 reduction potentials were about 100 mV negative of that measured in fluid electrolyte. Infrared studies demonstrated that the carboxylate forms of the sensitizers were present on the TiO_2 surface. Transformation of the electron-withdrawing ester groups to carboxylates is expected to shift the first reduction potentials of $M(bpy)_2(deebq)^{2+}$, $Ru(deebq)_2(bpy)^{2+}$, and $Ru(deebq)(bpy)(NCS)_2$ negative. However, the magnitude of the shift (∼100 mV) was not as large as one would anticipate based on solution studies, consistent with TiO_2 stabilization of the carboxylates.[63] The ∼90 mV negative shift observed after binding $Ru(bq)_2(deeb)^{2+}$ to TiO_2 is harder to rationalize as the first reduction is biquinoline based. To our knowledge, sensitizers that have the first ground- and excited-state reduction potentials below E_{cb} have never before been reported or investigated. It is for this reason that similar behavior has not been previously observed, Scheme 1.

Since electron transfer from TiO_2 to form the reduced sensitizers is energetically favored, eq 8, back electron transfer to the oxidized sensitizer must also be. This could form the excited state or the ground state, eqs 9 and 10.

$$e^-/TiO_2 + Ru^{II}(bpy)_2(dcbq)/TiO_2 \rightarrow Ru^{II}(bpy)_2(dcbq^-)^-/TiO_2 \quad (8)$$

$$e^-/TiO_2 + Ru^{III}(bpy)_2(dcbq)^+/TiO_2 \rightarrow Ru^{III}(bpy)_2(dcbq^-)^*/TiO_2 \quad (9)$$

$$e^-/TiO_2 + Ru^{III}(bpy)_2(dcbq)^+/TiO_2 \rightarrow Ru^{II}(bpy)_2(dcbq)/TiO_2 \quad (10)$$

The +3 formal oxidation state favors dcbq reduction by about 400 meV over the M(II) ground state, Table 2. For related Ru and Os compounds, the difference in reduction potentials between the excited and ground state is typically 300−500 meV.[64] No evidence for back electron transfer to generate an excited state was found in transient studies. This is attributed to the number of ground-state sensitizers relative to the number of oxidized sensitizers present at the interface. We estimate that there are about 500 sensitizers anchored to each TiO_2 nanoparticle. On average, pulsed light excitation promotes a few of these to excited states, only a fraction of which inject an electron into TiO_2. The injected electron has mobility and is statistically more likely to encounter a ground-state sensitizer than the oxidized sensitizer from which it originated.

Lateral Charge Transfer. Isoenergetic intermolecular charge transfer provides a mechanism by which charge can "hop" across the semiconductor surface. This allows encounters between the reduced and oxidized sensitizers to yield ground-state products. Previous researchers have shown that lateral charge transfer reactions can occur efficiently and rapidly with an applied bias.[27c,46,47] Control experiments with ZrO_2 substrates, for example, demonstrate that the semiconducting properties of TiO_2 are not responsible for the observed redox chemistry. Bonhote and co-workers have also shown that a percolation threshold exists for the oxidation of amines anchored to nanocrystalline TiO_2 thin films.[46]

In the present photo-initiated studies, we have modeled lateral charge transfer with the Kohlrausch−Williams−Watts function, which is a paradigm for transport in disordered media.[65,66] An advantage of this model is that the normalized data could be quantified with only two variables; β, which is inversely related to the width of an underlying Levy distribution of rate constants, and k, which is the rate constant at the maximum amplitude of the distribution. The average rate constants for a large number of samples were found to be $(8 \pm 5) \times 10^5\ s^{-1}$. The β values varied between 0.2 and 0.3 which corresponds to a highly skewed distribution of rates with a significant amplitude over 6 orders of magnitude.[66] A broad distribution would be expected if the donors and acceptors were located at variable distances

(56) Wang, P.; Wenger, B.; Humphry-Baker, R.; Moser, J. E.; Teuscher, J.; Kantlehner, W.; Mezger, J.; Stoyanov, E. V.; Zakeeruddin, S. M.; Gratzel, M. *J. Am. Chem. Soc.* **2005**, *127*, 6850.
(57) (a) Redmond, G.; Fitzmaurice, D. *J. Phys. Chem.* **1993**, *97*, 1426. (b) Enright, B.; Redmond, G.; Fitzmaurice, D. *J. Phys. Chem.* **1994**, *98*, 6195. (c) Redmond, G.; Grätzel, M.; Fitzmaurice, D. *J. Phys. Chem.* **1993**, *97*, 6951. (d) Boschloo, G.; Fitzmaurice, D. *J. Phys. Chem. B* **1999**, *103*, 2228. (e) Boschloo, G.; Fitzmaurice, D. *J. Phys. Chem. B* **1999**, *103*, 7860.
(58) Watson, D. F.; Meyer, G. J. *Coord. Chem. Rev.* **2004**, *248*, 1391.
(59) Clifford, J. N.; Opalomeras, E.; Nazeerudding, Md. K.; Graztel, M.; Nelson, J.; Long, N. J.; Durrant, J. R. *J. Am. Chem. Soc.* **2004**, *126*, 5225.
(60) Kuciauskas, D.; Freund, M. S.; Gray, H. B.; Winkler, J. R.; Lewis, N. S. *J. Phys. Chem. B* **2001**, *105*, 392.
(61) Nelson, J. *Phys. Rev. B* **1999**, *59*, 15374.
(62) Hasselmann, G. M.; Meyer, G. J. *J. Phys. Chem. B* **1999**, *103*, 7671.
(63) (a) Wolfbauer, G.; Bond, A. M.; Deacon, G. B.; MacFarlane, D. R.; Spiccia, L. *J. Am. Chem. Soc.* **2000**, *122*, 130. (b) Nazeeruddin, Md. K.; Zakeeruddin, S. M.; Humphry-Baker, M. J.; Liska, P.; Vlachopoulos, V. S.; Fischer, C.-H.; Grätzel, M. *Inorg. Chem.* **1999**, *38*, 6298.
(64) Kalyanasundaram, K. Photochemistry of Polypyridine and Porphyrin Complexes; Academic Press: London, 1992.
(65) (a) Kohlrausch, R. *Ann.* **1847**, *5*, 430. (b) Williams, G.; Watts, D. C. *Trans. Faraday Soc.* **1971**, *66*, 80.
(66) (a) Linsey, C. P.; Patterson, G. D. *J. Chem. Phys.* **1980**, *73*, 3348. (b) Majumdar, C. K. *Solid State Commun.* **1971**, *9*, 1087.

from each other. The long approximately millisecond lifetimes could correspond to redox equivalents generated on different TiO_2 nanocrystals for example.

A disadvantage of the KWW model is that it does not provide molecular insights into the recombination mechanism(s). An issue that naturally arises concerns which charges move faster, the electrons or the "holes". Hole transfer involves the metal t_{2g} orbitals while the biquinoline π^* orbitals mediate lateral electron transfer. For $Ru(bpy)_3^{2+}$ in fluid acetonitrile solution, the $Ru^{III/II}$ self-exchange rate constants are 2×10^9 M^{-1} s^{-1} and the $Ru^{2+/+}$ constants are 8×10^8 M^{-1} s^{-1}.[67,68] The high self-exchange rate constants have previously been discussed and reflect low intrinsic barriers to electron transfer.[69] However, the rate constants may be very different at the interface where the reorganization terms are expected to differ. To investigate this issue, the reduction and oxidation of the surface bound sensitizers were quantified by chronoabsorption measurements.[46−48] The potential of the sensitized TiO_2 films were stepped positive of the $Ru^{III/II}$ potential (or negative of the $Ru^{2+/+}$ potential), and the oxidation (reduction) of the surface bound sensitizers was monitored spectroscopically. With this approach, reduction was consistently found to occur on a seconds time scale, while oxidation required minutes. Diffusion constants abstracted from these data were consistently an order of magnitude larger for reduction. The energetic proximity of the first reduction potential with the conduction band edge suggests that TiO_2 may mediate the intermolecular electron transfer.

The possible role TiO_2 conduction band states may play in the electrochemical reduction of hemes and photochromic dyes has previously been suggested.[70−72] Sugihara and co-workers have also reported evidence that diimine ligands with low-lying π^* orbitals can mediate back electron transfer from TiO_2 to triiodide in regenerative solar cells.[73] Similar behavior has been reported more recently by Bignozzi.[74] Our ability to observe an injected electron fully localized and "trapped" on a ligand supports this general idea. At issue is the energetic position of the conduction band relative to the sensitizer π^* orbitals. In neat acetonitrile, the conduction band states clearly reside $>kT$ above the first reduction potential. However, when $LiClO_4$ was added to the external acetonitrile, the ligand based reduction potential and E_{cb} became more energetically proximate. At high $[Li^+]$, quenching of the MLCT excited state was apparent and photoinduced sensitizer reduction was not observed. This indicates that the sensitizer π^* orbitals and E_{cb} are energetically proximate and can be tuned relative to one another. Thus a TiO_2 mediated intermolecular electron transfer mechanism, either through a Boltzmann population of conduction band states or a superexchange type mechanism, is a reasonable explanation for the rapid reduction of the sensitizers anchored to TiO_2.[75] The $M^{III/II}$ potentials, on the other hand, are almost 2 eV positive of the conduction band, and a purely localized "hopping" mechanism must be operative for intermolecular "hole" transfer.

Conclusions

Photoinduced electron transfer reactions that store energy in excess of thermally equilibrated excited states have been realized for the first time. The approach described is general. Indeed one can envision exploiting this behavior in a variety of arrangements that employ semiconductor nanoparticles as (1) acceptors of electrons from vibrationally hot excited states and (2) conduits for electron transport to remote acceptors. In favorable cases, about 90% of the energy of an absorbed green photon and 93% of the energy of an absorbed red photon were converted to long-lived charge separated states. A disappointing aspect of the current work was the low yields that could not be optimized above 50%. This was clearly due to inefficient electron injection. While the factors that control ultrafast charge separation in these heteroleptic compounds remain unknown, it is encouraging to note that researchers have found conditions where ultrafast injection from related sensitizers are quantitative.[9,50] A significant challenge for future research is to couple these ultrafast charge separation processes with catalysts that can utilize the excess energy to drive fuel forming and environmentally friendly reactions. Studies of this type are underway in our laboratories.[76]

Acknowledgment. The Division of Chemical Sciences, Office of Basic Energy Sciences, Office of Energy Research, U.S. Department of Energy are gratefully acknowledged for research support. The authors thank Amy A. Narducci Sarjeant for help with the crystallographic data.

Supporting Information Available: Crystallographic data as CIF files. This material is available free of charge via the Internet at http://pubs.acs.org.

JA060470E

(67) (a) Chou, M.; Creutz, C.; Sutin, N. *J. Am. Chem. Soc*. **1977**, *99*, 5615. (b) Young, R.; Keene, R. *J. Am. Chem. Soc.* **1977**, *99*, 2468.
(68) (a) Motten, A. G.; Hanck, K.; DeArmond, M. K. *Chem. Phys. Lett.* **1981**, *79*, 541. (b) Heath, G. A.; Yellowless, L. J.; Braterman, P. S. *Chem. Phys. Lett.* **1982**, *92*, 646.
(69) Sutin, N.; Creutz, C. *Adv. Chem. Ser.* **1978**, *168*, 1.
(70) Wang, Q.; Zakeeruddin, X. M.; Cremer, J.; Bauerle, P.; Humphry-Baker, R.; Grätzel, M. *J. Am. Chem. Soc.* **2005**, *127*, 5706.
(71) Biancardo, M.; Argazzi, R.; Bignozzi, C. A. *Inorg. Chem.* **2005**, *44*, 9619.
(72) Obare, S. O.; Ito, T.; Meyer, G. J. *Environ. Sci. Technol.* **2005**, *39*, 6266.
(73) Yanagida, M.; Yamaguchi, T.; Kurashige, M.; Hara, K.; Katoh, R.; Sugihara, H.; Arakawa, H. *Inorg. Chem.* **2003**, *42*, 7921.
(74) Altobello, S.; Argazzi, R.; Caramori, S.; Contado, C.; Da Fre, S.; Rubino, P.; Chone, C.; Larramona, G.; Bignozzi, C. A. *J. Am. Chem. Soc.* **2005**, *127*, 15342.
(75) Davis, W. B.; Svec, W. A.; Ratner, M. A.; Wasielewski, M. R. *Nature* **1998**, *396*, 60.
(76) Obare, S. O.; Ito, T.; Meyer, G. J. *J. Am. Chem. Soc.* **2006**, *128*, 712−713.